Investigation of Problems in Thermal Convection

J. R. HERRING

Goddard Institute for Space Studies, New York, N. Y.

(Manuscript received 5 April 1963)

ABSTRACT

The thermal convection equations for a thin layer of fluid are solved numerically as an initial value problem. The calculations include only those nonlinear terms which have the form of an interaction of a fluctuation in the velocity and temperature with the mean temperature field. In the present calculations, the velocity and temperature fluctuations have one horizontal wave number, and satisfy free boundary conditions on two conducting horizontal surfaces.

The computed steady state velocity and temperature amplitudes show many of the observed qualitative features. In particular, the experimentally observed boundary layering of the mean temperature field is correctly reproduced, and, at large Rayleigh number, the total heat transport is found to be proportional to the cube root of the Rayleigh number, provided the fluctuating temperature and velocity amplitudes have that horizontal wave number which maximizes the total heat transport. However, the heat transport found here for free boundaries is about three times the experimental value for rigid boundaries. The mean temperature gradient can become negative near the boundaries for large Rayleigh numbers and large horizontal scale motions.

The linear stability of the system is also investigated, and it is concluded that the stable solutions for all Rayleigh numbers investigated $(R<10^6)$ have horizontal wave numbers which very nearly maximize the total heat transport. The stability study also indicates regions in which two or more horizontal wave numbers are required to support convection.

1. Introduction

This paper describes the results of a numerical investigation of the thermal convection equations for a thin layer of fluid confined between two plates on which free boundary conditions are employed. Our theoretical procedure is to include only those nonlinear terms which describe the interaction of the mean temperature with velocity and temperature fluctuations. That is, those terms responsible for eddy viscosity and eddy conductivity effects on the turbulence itself are omitted. The above eddy terms (hereafter referred to as fluctuating self-interactions) are discarded in a physically consistent manner, so that no unrealistic behavior results from their omission.

The motivation for this research is to discover quantitatively to what extent the turbulent convection problem can be comprehended without the fluctuating self-interactions. The system of equations obtained by deleting these terms corresponds to closing the hierarchy of moment equations at the first nontrivial level by discarding third order cumulants. The resulting system of equations is complete and involves no empirical parameters. Moreover, the gross energetics of the flow are preserved.

The method of numerical solution consists in integrating the Fourier amplitudes of the velocity and temperature fields forward in time until the steady state is achieved. This procedure has the advantage of assuring

the stability of the final state provided a sufficient range of initial data is sampled. The present calculations, carried out on an IBM 7090 computer, contain one horizontal wave number and enough vertical wave numbers to ensure the elimination of truncation errors. In the numerical analysis, we have set the Prandtl number equal to unity. However, inspection of the equations which omit the fluctuating self-interactions shows that the heat transport is not a function of Prandtl number, if the system is steady.[1]

The calculated velocity and temperature fields show many of the qualitative features of the experimentally determined fields. In particular, at large Rayleigh number, R, the total heat transport is found to be proportional to $R^{\frac{1}{3}}$, provided the velocity and temperature fluctuation fields have that horizontal wave number which maximizes the heat transport. However, the heat transport found here for free-boundary conditions is three times the experimental value for rigid-boundary conditions. Preliminary numerical studies of the rigid-boundary problem indicate that for large Rayleigh numbers $(R\sim10^6)$ the heat transport is about a factor of 2.3 smaller than that for free-boundaries and therefore approximately 50 per cent higher than the experiment. Thus, it appears that the boundary conditions are quite important in producing the experimental heat

---

[1] For a discussion of the Prandtl number dependence of the heat transport for the complete system, see Kraichnan (1962a).

transport. The system has two additional failings: it turns out that the fluctuating amplitudes are steady in time and the horizontal plan form of the motions is indeterminate.

The mean temperature gradient at low R closely resembles the experimental temperature profiles. At large Rayleigh numbers $(R \sim 10^6)$, the gross features of the temperature profiles are correctly predicted by our system. The computed mean temperature gradients are large in a thin layer adjacent to the boundary and are quite small in the body of the fluid. The gradients near the boundary can become negative for motions of large horizontal scale, but remain positive for motions of a sufficiently small horizontal scale.

The stability of the steady state solutions against infinitesimal perturbation at other horizontal wave numbers is also investigated and the regions of instability are delineated. These results closely parallel perturbation results at low Rayleigh number and support the idea that the most stable solution is near the one transporting the most heat flux (Malkus and Veronis, 1958). A finite amplitude stability study, and the associated development of a several-horizontal-wave-number system to steady state will be the topic of a future investigation.

The idea that the important features of the convection problem are contained in the system which omits the fluctuating self-interactions is implicit in the theory of convection advanced by Malkus (1954). In the original formulation of his theory, Malkus sought a maximum for the heat transport subject to the constraint that the temperature gradient be positive, and that there be a smallest scale of motion participating in the advective heat transport. The smallest scale is supposed to be determined by the requirement that it be marginally stable in the presence of the mean temperature gradient occurring in the fluid. The smallest scale so determined furnished a cut-off in the cosine representation of the mean temperature gradient. The assumption that the heat transport was maximum under the above constraints then led to an explicit form for the temperature gradient.

A more recent formulation of the Malkus theory by Spiegel (1962) replaces the cosine representation of the temperature gradient by an expansion in terms of the set of eigenfunctions, which are marginally stable on the mean temperature gradient. This version of the Malkus theory is exactly equivalent to the system considered here, provided the horizontal scale of the motions is such that the mean temperature gradient is everywhere positive. In this sense, our numerical results contain, as a special case, the exact solutions to the Malkus theory for one horizontal wave number and free boundaries.

In this connection, a comparison of our computed temperature gradients with the predictions of the

Malkus theory is relevant. In making this comparison, we must keep in mind that the system considered here is explicitly confined to only one horizontal wave number, whereas Malkus makes no explicit references to the nature of the horizontal-wave-number spectrum. We do not confirm the z^{-2} law for the gradient outside the boundary layer as predicted by Malkus, nor do we find a sharp cut off in the cosine spectrum of the temperature gradients.

At low Rayleigh numbers $(R < 2000)$ our numerical results are in agreement with the calculations of Malkus and Veronis (1958) and Kuo (1961), who have obtained perturbation solutions to the convection equations. A procedure similar to ours has been used by Saltzman (1961) in studying the complete convection equations for $R \lesssim 6000$. Our approach differs from his in that we are able to allow very many vertical modes to be excited, whereas his results are limited to one vertical mode. Our results indicate that it is essential to allow many more vertical modes than horizontal modes, if large truncation errors are to be avoided. Thus, at $R = 4000$, 10 vertical modes must be included to obtain realistic temperature profiles.

2. Theory

a) The equation of motion and boundary conditions. We consider a thin layer of fluid confined between two infinitely conducting plates located at $z = 0$ and $z = d$. The lower plate is maintained at zero degrees, and the top plate at a temperature $-T_0$, on an arbitrary temperature scale. The direction of gravity is specified by the unit vector $-\mathbf{k}$. The equations appropriate for our system are the Boussinesq approximations to the Navier-Stokes equations (Chandrasekhar, 1961, p. 16). We shall write these equations in a form in which the velocity and temperature ($\mathbf{v}$ and T) as well as the coordinate and time ($\mathbf{r}$ and t) are nondimensional. The only parameters entering the equations are then the Rayleigh number, R, and the Prandtl number, σ. The equations are

$$\nabla \cdot \mathbf{v} = 0, \tag{1}$$

$$\left(\frac{1}{\sigma}\frac{\partial}{\partial t} - \nabla^2\right)\nabla^2 \mathbf{v} = -\frac{1}{\sigma}\nabla \times (\nabla \times (\mathbf{v} \cdot \nabla \mathbf{v})) + R\nabla \times (\nabla \times \mathbf{k}T), \tag{2}$$

$$\left(\frac{\partial}{\partial t} - \nabla^2\right)T = -\nabla \cdot (\mathbf{v}T). \tag{3}$$

Equation (2) is actually the double curl of the momentum equation, and hence the pressure variable is absent. The nondimensional variables are related to the dimensional ones (denoted by primes) in the following way:

$$\mathbf{v} = \frac{d}{\kappa}\mathbf{v}',$$

$$T = T'/d,$$

$$\mathbf{r} = \mathbf{r}'/d,$$

$$t = \frac{\kappa}{d^2}t'.$$

Here κ is the thermometric diffusivity of the fluid.

The boundary conditions on the velocity field are derived from the requirement that the fluid exert no shear on the confining plates. This, together with the continuity equation, implies that all even derivatives of the vertical velocity, w, vanish on the boundary. In the nondimensional notation the boundary conditions are

$$\frac{\partial^m}{\partial z^m}w(0,t) = \frac{\partial^m}{\partial z^m}w(1,t) = 0, \quad m = 0, 2, 4, \cdots \quad (4)$$

and

$$T(0,t) = 0; \quad T(1,t) = -1. \quad (5)$$

b) Discard of the fluctuating self-interactions. It is convenient to resolve the temperature field into a horizontal mean plus a fluctuating part;

$$T = -z + \psi(z,t) + \theta(\mathbf{r},t). \quad (6)$$

Here, $\psi(z,t)$ is a horizontally averaged distortion of the conduction state and $\theta(\mathbf{r},t)$ is the fluctuation of the temperature from its distorted value. In view of the boundary condition (5), and the interpretation of θ as a fluctuation from the horizontal mean, we may write

$$\psi(0,t) = \psi(1,t) = 0 \quad (7)$$

$$\theta(x,y,0,t) = \theta(x,y,1,t) = \bar{\theta} = 0. \quad (8)$$

The bar on (8) indicates an average over the horizontal. We now introduce (6) into (1), (2), and (3) and subtract from each of the resulting equations their respective horizontal mean. We find

$$\left(\frac{1}{\sigma}\frac{\partial}{\partial t} - \nabla^2\right)\nabla^2 w = R\nabla_1^2\theta + \frac{1}{\sigma}\{\nabla \times \nabla \times (\mathbf{v}\cdot\nabla\mathbf{v})\}_z,$$

$$\left(\frac{\partial}{\partial t} - \nabla^2\right)\theta = \left(1 - \frac{\partial\psi}{\partial z}\right)w - \nabla\cdot(v\theta - \overline{\mathbf{k}w\theta}),$$

$$\left(\frac{\partial}{\partial t} - \frac{\partial^2}{\partial z^2}\right)\psi = -\frac{\partial}{\partial z}\overline{w\theta},$$

where

$$\nabla_1^2 = \frac{\partial^2}{\partial x^2} + \frac{\partial^2}{\partial y^2}.$$

There are two more equations, for the x- and y-components of the velocity field, but these are not necessary for our problem. The last terms in the equations above for w and θ have the form of a deviation of a bilinear fluctuating quantity from its horizontal mean (fluctuating self-interaction). By discarding these terms we obtain the system to be investigated;

$$\left(\frac{1}{\sigma}\frac{\partial}{\partial t} - \nabla^2\right)\nabla^2 w = R\nabla_1^2\theta, \quad (9)$$

$$\left(\frac{\partial}{\partial t} - \nabla^2\right)\theta = \beta w, \quad (10)$$

$$\left(\frac{\partial}{\partial t} - \frac{\partial^2}{\partial z^2}\right)\psi = -\frac{\partial}{\partial z}\overline{w\theta}, \quad (11)$$

where

$$\beta(z) = 1 - \frac{\partial\psi}{\partial z} = -\frac{\partial}{\partial z}\bar{T}.$$

The significance of omitting fluctuating self-interaction can be expressed formally by examining the hierarchy of moment equations obtained from (1)–(3). By multiplying equations (2) and (3) by $v(t')$ and $T(t')$ and ensemble-averaging the appropriate sums of the resulting equations, we obtain the time evolution equations for the correlation coefficients $\langle v_i v_j \rangle$, and $\langle v_i T' \rangle$, and $\langle TT' \rangle$. These equations couple the above second order moments to the transfer terms, which are cubic in $\mathbf{v}$ and T.

Since the system contains a non-vanishing first-order moment, ψ, the transfer terms contain both correlated third-order moments (cumulants) and products of first order moments with second-order moments. The discarding of the fluctuating self-interaction then corresponds to closing the system of moment equations by discarding the third order cumulants.[2] In the absence of mean fields this procedure would be empty.

We must now verify that our procedure of deleting third-order cumulants does not lead to physically unrealistic results. For our procedure to be acceptable, the system of (9), (10) and (11) must obey the conservation laws associated with the complete set of convection equations, and they must be free from unphysical consequences of the sort recently discussed by Ogura (1962), for a similar problem in isotropic turbulence. Ogura has demonstrated that the assumption of zero fourth-order cumulants and nonzero third-order cumulants is in-

---

[2] Discarding third order cumulants is quite different from discarding third order *moments*. The latter procedure has as a consequence that no steady state nontrivial amplitudes exist. For an investigation of the dynamics of decay for zero third-order moments see Deissler (1962).

compatible with a positive energy spectrum for all wave numbers.[3]

With regard to the last point, it should be noted that the positive definite character of the kinetic energy wave number spectrum and the spectrum for the square of the temperature field follows directly from the fact that it is possible to write the equations which delete third order cumulants in terms of amplitudes rather than moments. We observe that the amplitude (9), (10) and (11) all have real coefficients; hence, the square of any amplitude will remain positive for all time if the amplitude is initially a real number.

The conservation of entropy and kinetic energy are also preserved without the fluctuating self-interactions. By multiplying (10) by θ, (11) by ψ, and adding, we obtain after integrating over the entire volume of the fluid, the equation of conservation of entropy,

$$\frac{1}{2}\frac{\partial}{\partial t}\{|\theta|+|\psi|^2\}_v+\{|\nabla\psi|^2+|\nabla\theta|^2\}_v=\{w\theta\}_v. \qquad (12)$$

Here the v subscript indicates an integration over the entire volume of the system.

We observe that equation (12), with a corresponding one for the conservation of the kinetic energy (Malkus and Veronis, 1958, p. 228) of the flow are exactly the same as those with the fluctuating self-interaction included. Contributions from the latter may be reduced to surface integrals which vanish.

c) Fourier decomposition of the equations. It is convenient to work with the Fourier components of (9)–(11) rather than their space-variable form. The free boundary conditions make the sine series appropriate. We therefore write:

$$w(\mathbf{r},t)=\sum_{n,\alpha} f_\alpha(x,y)w_n{}^\alpha \sin n\pi z,$$

$$\theta(\mathbf{r},t)=\sum_{n,\alpha} f_\alpha(x,y)\theta_n{}^\alpha \sin n\pi z,$$

$$\psi(z,t)=\sum_n \psi_n \sin n\pi z.$$

Here $f_\alpha(x,y)$ is an arbitrary set of orthonormal functions generated by the operator $\nabla_1{}^2$, and obeying appropriate periodic boundary conditions in the horizontal:

$$\nabla_1{}^2 f_\alpha(x,y)= -\pi^2\alpha^2 f_\alpha(x,y)$$

and

$$|\overline{f_\alpha f_{\alpha'}}|^2=\delta_{\alpha\alpha'}.$$

Introducing the above representation into (9), (10) and (11) gives the following set of equations for the amplitudes w_n, θ_n, and ψ_n:

[3] For a complete discussion of the cumulant discard approximations, see Kraichnan (1962a).

$$\left(\frac{1}{\sigma}\frac{\partial}{\partial\tau}+n^2+\alpha^2\right)\omega_n{}^\alpha=\frac{\lambda\alpha^2}{n^2+\alpha^2}\theta_n{}^\alpha, \qquad (13)$$

$$\left(\frac{\partial}{\partial\tau}+n^2+\alpha^2\right)\theta_n{}^\alpha$$
$$=\omega_n{}^\alpha-\frac{\pi}{2}\sum_{p=1} p\psi_p(\omega_{n+p}{}^\alpha+\sigma(n-p)\omega^\alpha{}_{|n-p|}), \qquad (14)$$

$$\left(\frac{\partial}{\partial\tau}+n^2\right)\psi_n$$
$$=\frac{\pi n}{2}\sum_{p=1}\sum_\alpha \omega_p{}^\alpha(\theta_{n+p}{}^\alpha+\sigma(p-n)\theta^\alpha{}_{|n-p|}), \qquad (15)$$

where

$$\lambda=R/\pi^4,$$
$$\tau=\pi^2 t,$$
$$\omega_n=w_n/\pi^2,$$

and

$$\sigma(x)=1, \qquad x>0$$
$$=0, \qquad x=0$$
$$=-1, \qquad x<0.$$

Manipulation of the convolution terms in (14) and (15) is aided by the following identities:

$$\sum_p A_p(B_{n+p}+\sigma(n-p)B_{|n-p|})=\sum_p B_p(A_{|n-p|}-A_{n+p}),$$

and

$$\sum_p A_p(B_{n+p}+\sigma(p-n)B_{|p-n|})$$
$$=\sum_p B_p(A_{n+p}+\sigma(p-n)A_{|p-n|}).$$

There are two conservation equations derivable from (14) and (15). The first is the Fourier representation of (12) for conservation of entropy. The other is the equation that partitions the total heat flux between conduction and convection; it is derived by multiplying (15) by $1/n$ and summing over n. We find

$$\sum_n\left(\frac{1}{n^2}\frac{\partial}{\partial t}+1\right)\beta_n=\frac{\pi^2}{2}\sum_{n,\alpha}\omega_n{}^\alpha\theta_n{}^\alpha, \qquad (16)$$

where

$$\beta_n=-\pi_n\psi_n.$$

Here the β_n's are the cosine transform of the mean temperature gradient. In the statistically steady state, (16) is the equation for the total heat flux, which is a constant of motion for the system. We now introduce a quantity $N(t)$, the total heat flux at the lower boundary:
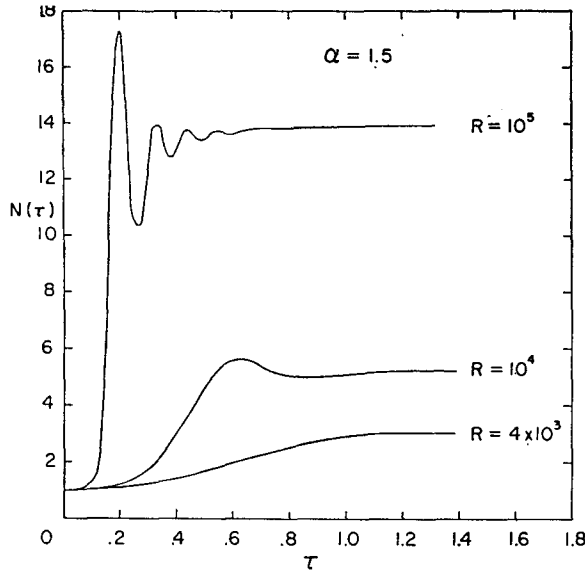
$$N(t)=1+\sum_1^\infty \beta_n(t). \qquad (17)$$

FIG. 1. Time development of the total heat flux, $N(\tau)$ for $R=4\times10^3$, 10^4, 10^5 and $\alpha=1.5$. The system is in the conduction state at $\tau=0$, with all fluctuating amplitudes except w_1 equal to zero.

FIG. 2. $4.22\times10^{-2}w$ and 4.07θ for $R=4\times10^3$ and $\alpha=0.8$.

If the mean amplitudes are constant,

$$N=1+\frac{\pi^2}{2}\sum_{n,\alpha}\omega_n{}^\alpha\theta_n{}^\alpha.$$

In our units, the conduction state transports unit heat flux and this equation is the nondimensional form for the familiar equation for the total heat flux.

d. Structure of the equation. Before proceeding to the numerical results, we give a brief resumé of the pertinent qualitative features of the system defined by (13), (14) and (15). First of all, we note that the horizontal wave numbers, α, are coupled only in their effect on the mean temperature field ψ. This interaction occurs diagonally in the sense that each α interacts only with itself. As a consequence there is a degeneracy in the horizontal plan form of the motion; the system is insensitive to the particular cell shape. Moreover, the number of α's is also indeterminate. The simplest situation is to have a single α support the motion and we investigate only this case here.

A single α will give nontrivial answers for the amplitudes w and θ only if it lies within a certain range. The range of α which will *not* support convection is obtained by assuming w and θ to be small, and demanding that they subsequently decay. If w and θ are small, ψ will be small to second order and our question is equivalent to that of marginal stability (See Chandrasekhar, 1961, p. 35). The system then will not support convection if

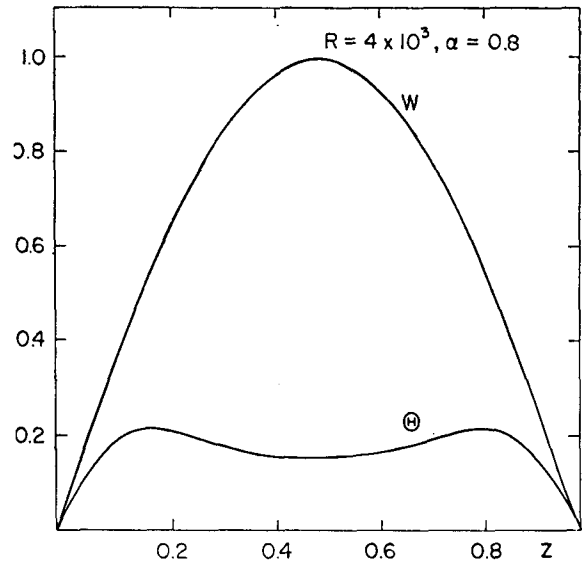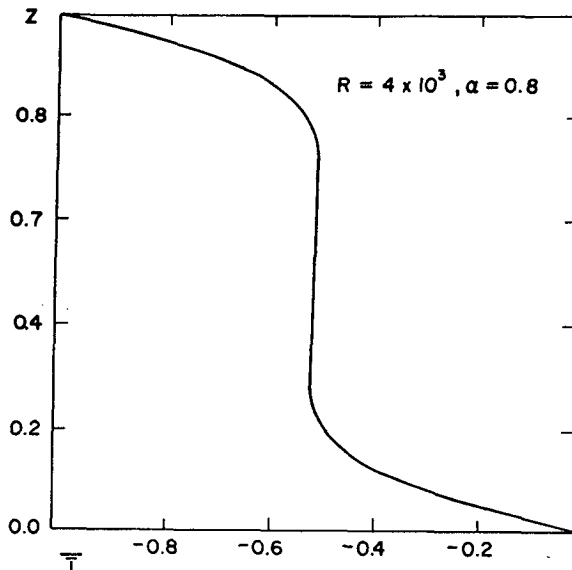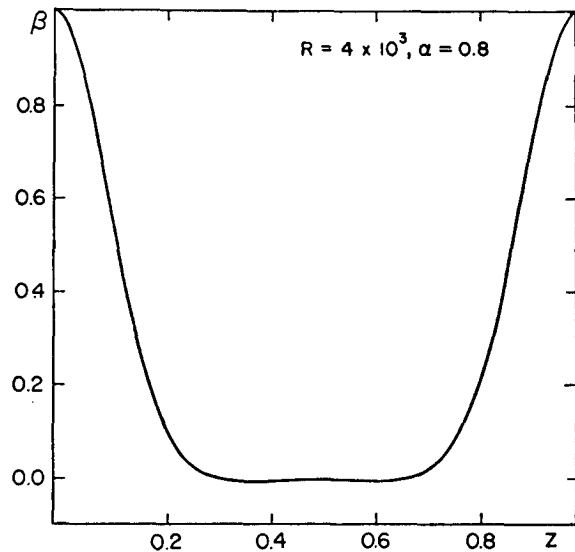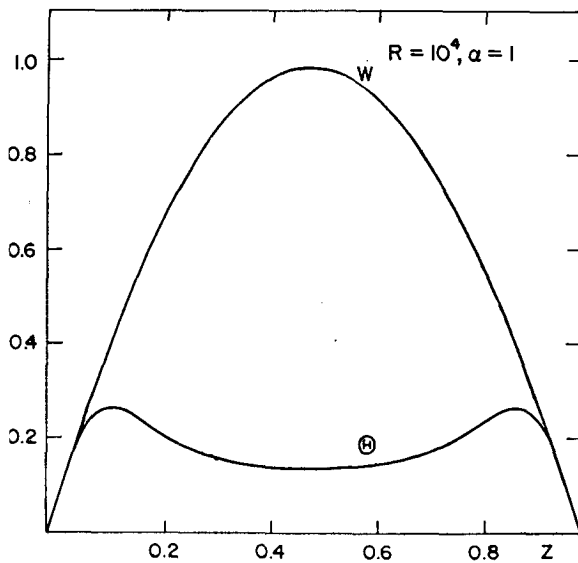$$\frac{(1+\alpha^2)^3}{\alpha^2}\geq\frac{R}{\pi^4}. \tag{18}$$

Conversely, we assume that the steady state values of w and θ will be nonzero if α lies in the range complementary to (18).

The time behavior of the system is complicated by nonlinear effects. In the approach to the steady state, our numerical results indicate that the system executes overdamped oscillations with an ever increasing period of oscillation. This last remark is understandable since w and θ become marginally stable as $t\to\infty$.

If the mean field, ψ, is statistically steady as $t\to\infty$, we may use a theorem of Spiegel (1962, p. 196) to show that w and θ are independent of time. Spiegel has shown that the principle of exchange of stability is valid (for free boundaries) in the presence of the mean gradient corresponding to the steady state solution to the mean temperature field given by (15). This implies that the growth rates for the appropriate eigen-function expansion for w and θ must all be zero in order for there to be a statistically steady state.

3. Numerical procedure

In performing the numerical integration, we discard from the onset those Fourier amplitudes which will be zero in the steady state. We assume that the steady state amplitudes ω, θ and β have even parity about the mid-point $z=\frac{1}{2}$. This means that the even sine modes of ω and θ, and the odd cosine modes of β will have zero amplitude in the steady state. We therefore put their initial values equal to zero. The equations of motion (13), (14) and (15) then imply that the odd parity modes will remain zero for all subsequent time. Defining $\tilde\beta_n=\beta_{2n}$, we may rewrite (14) and (15) in a more con-

FIG. 3(a). Mean temperature, $\bar{T}(z)$, for R=4×10³ and α=0.8.

FIG. 3(b). Mean gradient, $\beta(z)$, for R=4×10³ and α=0.8. $\beta(z)$ is normalized by the total heat transport, N=3.92.

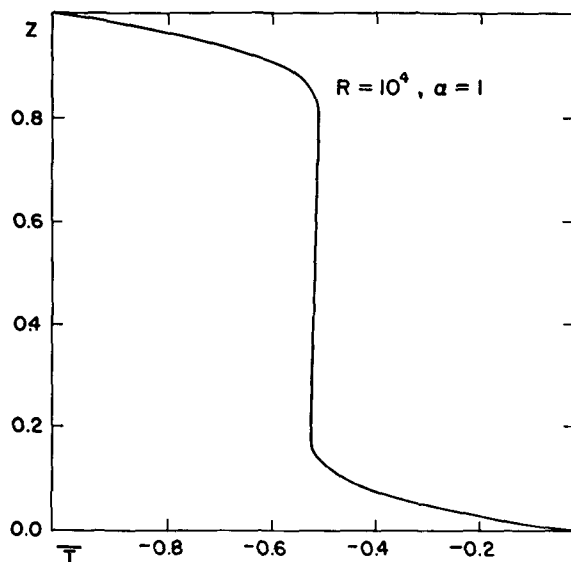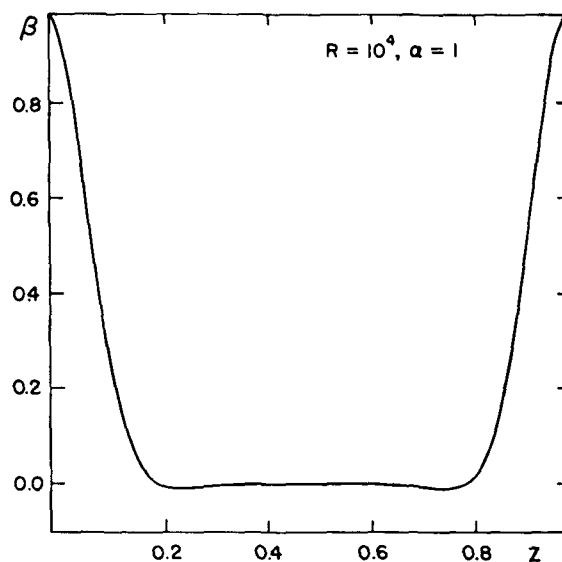FIG. 4. 2.05×10⁻²w and 5.16θ for R=10⁴ and α=1.0.

venient form:

$$\left(\frac{\partial}{\partial\tau}+n^2+\alpha^2\right)\theta_n$$

$$=\omega_n+\tfrac{1}{2}\sum_{p=1}^{\infty}\bar{\beta}_p(\omega_{n+2p}+\sigma(n-2p)\omega_{|n-2p|}), \quad (14')$$

$$\left(\frac{\partial}{\partial\tau}+4n^2\right)\bar{\beta}_n$$

$$=-2\pi^2 n^2\sum_{p=1}^{\infty}\omega_p(\theta_{2n-p}+\sigma(p-2n)\theta_{|2n-p|}). \quad (15')$$

Here, we have dropped the α superscript since we are interested in the system containing only one α. Equation (13) remains unchanged and the total heat flux is computed from (17).

Our procedure for integrating these equations is to assign an initial set of amplitudes to ω_n, θ_n, $\bar{\beta}_n$, and allow the system to evolve to the steady state. In doing so, we must truncate the infinite set of equations. Our procedure in this matter is to set all amplitudes ω_n, θ_n, $\bar{\beta}_n$ of index greater than a certain integer, n_0, equal to zero. This method of truncation guarantees exact conservation of heat flux and entropy for the abbreviated system. Since ω_1 is generally large and the θ_n's decrease rather slowly, we see from (15') that amplitudes for $\bar{\beta}_n$ above $n_0/2$ will have significant truncation errors. Truncation errors are assumed to be negligible if increasing n_0 does not appreciably alter the value of the total heat transport. The total number of $\bar{\beta}_N$ modes included in these calculations ranged from 20 modes at R=4000 to 80 modes at R=10⁶. The errors in the total heat transport due to the above are estimated to be less than one part in 10³.

The integration forward in time was continued until constancy of heat flux (16) and entropy (12) was achieved to one part in 10⁴. The time, in τ units, necessary to achieve this ran from ~1.4 at R=4×10³ to 0.3 at R=10⁶. At high Rayleigh numbers, this criterion was not too satisfactory, since constancy of heat flux and entropy were achieved long before the amplitudes w and θ became steady. For these cases, it was necessary to check the time derivatives of the slowest evolving amplitudes, w_1 and θ_1. The system was observed to be steady if the derivative of w_1 was less than 2 per cent of w_1.
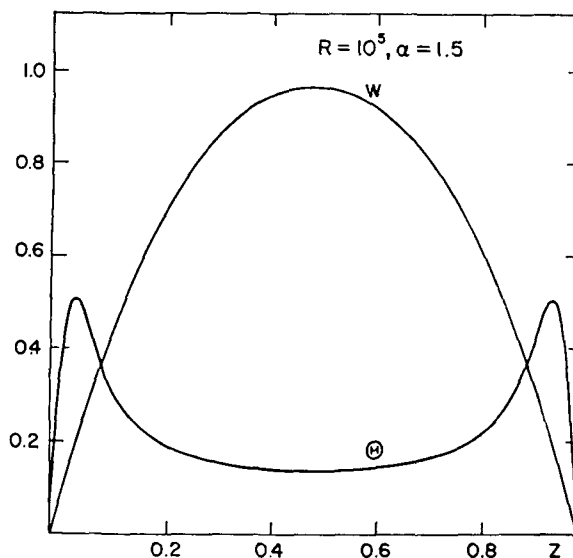
FIG. 5(a). Mean temperature, $\bar{T}(z)$, for $R=10^4$ and $\alpha=1.0$.

FIG. 5(b). Mean gradient, $\beta(z)$, for $R=10^4$ and $\alpha=1.0$. $\beta(z)$ is normalized by the total heat transport, $N=5.82$.

Examples of the time evolution for the total heat transport $N(\tau)$ are given in Fig. 1, for $R=4\times10^3$, 10^4, 10^5 and $\alpha=1.5$. The system was started in the conduction state at $\tau=0$, with all fluctuating amplitudes ω_n and θ_n equal to zero, except ω_1, which has an initial value of unity. The convection is seen to develop initially by way of large oscillations, and to decay to the steady state with overdamped oscillations, whose period becomes increasingly larger. The time scale of the initial oscillations in these curves is of the order of the growth rate time in the conduction state.
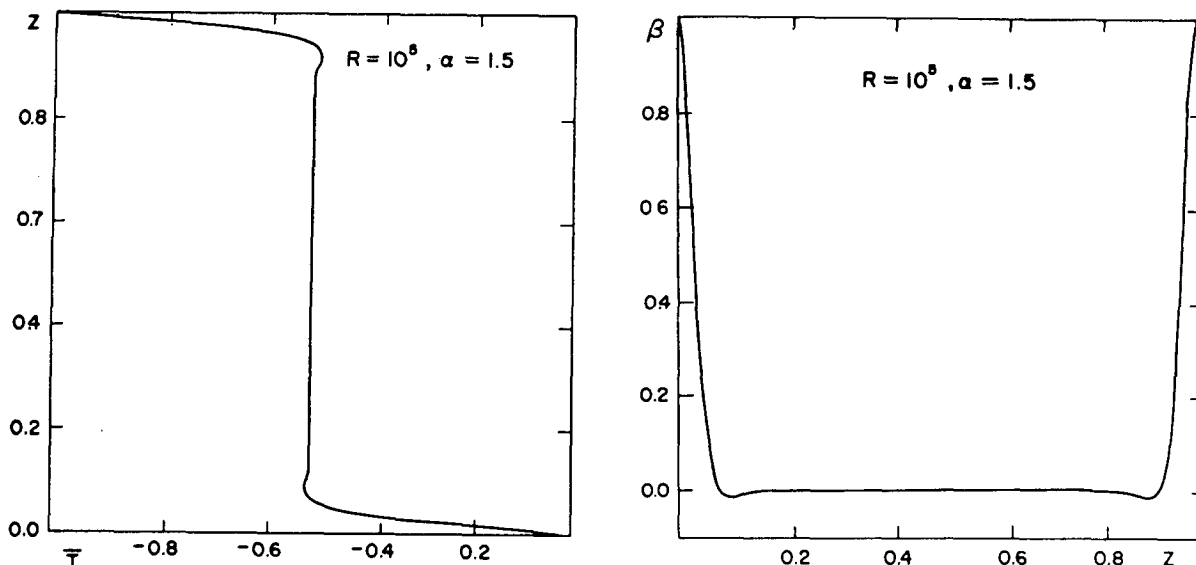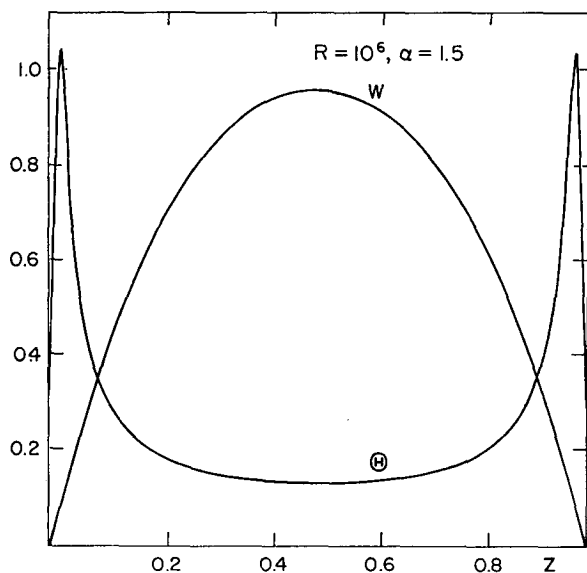
4. Discussion of results

The computed steady state amplitudes are shown in Figs. 2–13. The normalization for β, w and θ is given in the captions, while $\bar{T}(z)$ requires no normalization. The graphs of $\bar{T}(z)$ are in a reflected coordinate system to conform with an accepted procedure. The values of α in Figs. 2–9 were chosen so that the heat transport is very near its maximum. We now discuss in some detail the physical features of the steady state amplitudes ω, θ, β and $\bar{T}$.

a) The mean temperature $\bar{T}$, and mean gradient $\beta(z)$. The mean fields, $\bar{T}$ and β in Figs. 3, 5, 7, 9, 11 and 13 have an interesting behavior near the boundaries. At low Rayleigh number, these fields closely resemble the perturbation results of Markus and Veronis (1958), but the temperature gradient is slightly negative in the central region. As the Rayleigh number is increased, the negative temperature region collects closer to the boundary while in the central region, the temperature gradient becomes extremely small but positive.

FIG. 6. $4.33\times10^{-3}w$ and 9.42θ for $R=10^5$ and $\alpha=1.5$.

The negative temperature gradient boundary region is apparently produced by an overshoot phenomenon. These occur typically for motions of large horizontal scale (small α) and disappear for motion of small horizontal scale. (See Figs. 9, 11 and 13.) If the motion has a large horizontal scale, an element of fluid close to the lower plate moves in a region of high temperature for a relatively long time. When it eventually turns upward, it moves unchecked by eddy processes and penetrates the body of the fluid with an excessive heat flux. The mean gradient accommodates this motion by turning negative. The negative β region then checks the velocity field, so

FIG. 7(a). Mean temperature, $\bar{T}(z)$, for $R=10^5$ and $\alpha=1.5$.

FIG. 7(b). Mean gradient, $\beta(z)$, for $R=10^5$ and $\alpha=1.5$. $\beta(z)$ is normalized by the total heat transport, $N=13.82$.

FIG. 8. $8.98\times10^{-4}w$ and 19.4θ for $R=10^6$ and $\alpha=1.5$.

that the advective heat transport decreases toward the middle of the fluid. We see here evidence for the non-local property of the flow; if the Rayleigh criteria for convection were applicable locally, a negative β region would not persist in the steady state.

For motions of small horizontal scale (Figs. 11 and 13) the situation is somewhat different. In this case, an element absorbs little heat from the lower boundary region and loses it quickly by conduction because it belongs to a vertically elongated cell pattern. It also loses momentum by viscous drag, and attains its
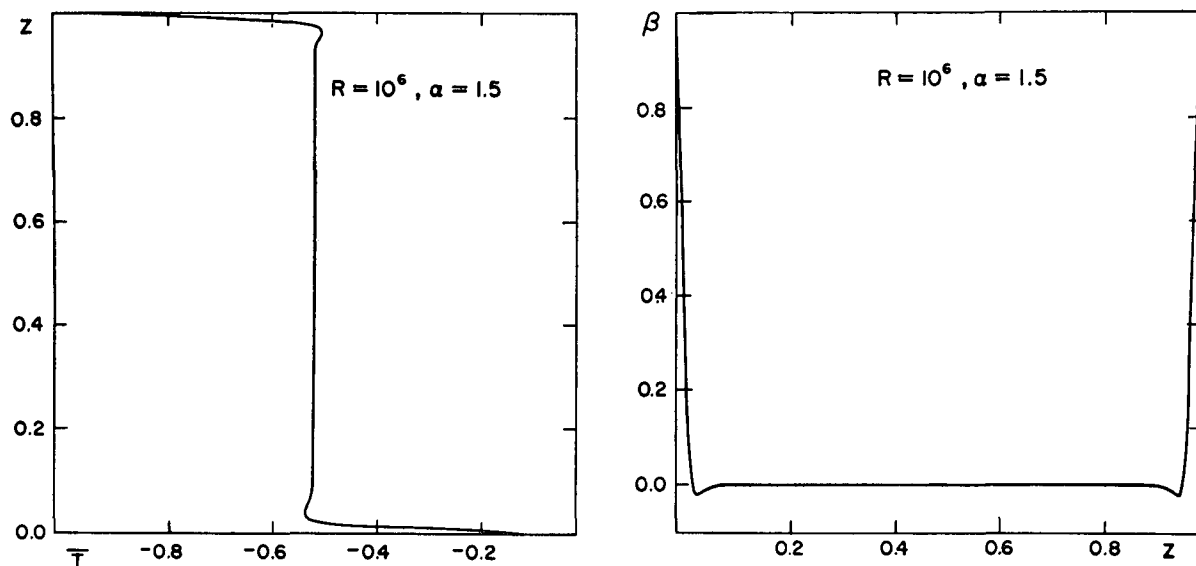
terminal velocity before reaching the central region of the fluid (see Figs. 10 and 12). To maintain constancy of heat flux the central region must conduct rather strongly, so that the mean gradient becomes large there.

b) Velocity and temperature fluctuations. The velocity and temperature fluctuation fields are shown in Figs. 2, 4, 6, 8, 10 and 12. We observe that the velocity fields, for all Rayleigh numbers, have an extremely large first mode. For example, at $R=4000$ (Fig. 2) w_1 represents 99 per cent of the total velocity amplitude, while at $R=10^6$ (Fig. 8) w_1 is 95 per cent of the total. On the other hand, the θ_n modes decrease rather slowly as n increases.

The above behavior of the ω_n and θ_n spectra displays the character of the nonlinear coupling in our system. Thus, the term $\omega_1\theta_{2n-1}$ tends to be the dominant contributor to $\bar{\beta}_n$ [see equation (15')] for reasonably small n. Conversely, terms of the form $\bar{\beta}_n\omega_1$ and $\bar{\beta}_{n-1}\omega_1$ tend to be the dominant contributors to θ_n [equation (14')]. The nonlinear coupling scheme in the equations of motion is therefore highly nondiagonal, as opposed to the case of isotropic turbulence.

The strong nondiagonal coupling in the system of Fourier modes is a result of the distortion of the mean temperature profile combined with the pressure and dissipative forces for incompressible flow. The above forces are directly responsible for the occurrence of sixth-order derivatives in the marginal stability problem, of which the steady state amplitudes ω and θ are solutions in the presence of the mean field β. If we solve for the velocity modes ω_n', in the presence of the mean gradient β, by using the iteration technique of Section 5, we see that the higher modes of ω_n are sup-

Fig. 9(a). Mean temperature, $\bar{T}(z)$, for $R = 10^6$ and $\alpha = 1.5$.

Fig. 9(b). Mean gradient, $\beta(z)$, for $R = 10^6$ and $\alpha = 1.5$. $\beta(z)$ is normalized by the total heat transport, $N = 31.48$.
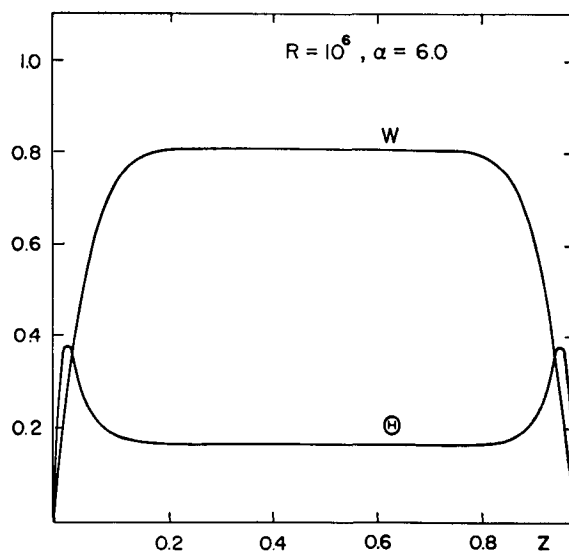
pressed by a factor $\sim n^{-6}$. For a reasonable β, this factor results in the higher ω_n modes making only a small contribution to ω.

c) *Temperature gradient spectrum.* The cosine spectrum of the mean temperature gradient, β, is given in Fig. 14 for $R = 10^4$, 10^5, 10^6 and $\alpha = 1.5$. We have connected the points with a smooth curve for the sake of clarity. We notice a tendency for the lower modes to saturate at $\beta_n = 2$, which corresponds to the small gradient outside the boundary layer. In fact, if $\beta_n = 2$ for all n, $\beta(z)$ is a δ function, and the gradient vanishes everywhere except at the boundary, where it becomes singular. At large Rayleigh numbers, the β_n spectrum is nearly Gaussian for small n, but decreases more rapidly at large n.

The tendency for the $\bar{\beta}_n$'s (for small n) to approach 2 as an upper bound is closely connected with the fact that the velocity field is marginally stable on the mean temperature gradient, β. This feature is brought out more clearly by examining the relation connecting the mean gradient field, $\bar{\beta}_n$ and the Rayleigh number R. Using the iteration method of Section V, we find

$$\frac{(1+^2)^3}{\alpha^2}\frac{\pi^4}{R} = 1 - \tfrac{1}{2}\beta_1 + \frac{1/4}{1-\tfrac{1}{2}\beta_1}\sum_1^\infty \frac{(1+\alpha^2)^3}{[(2n+1)^2+\alpha^2]^3}$$

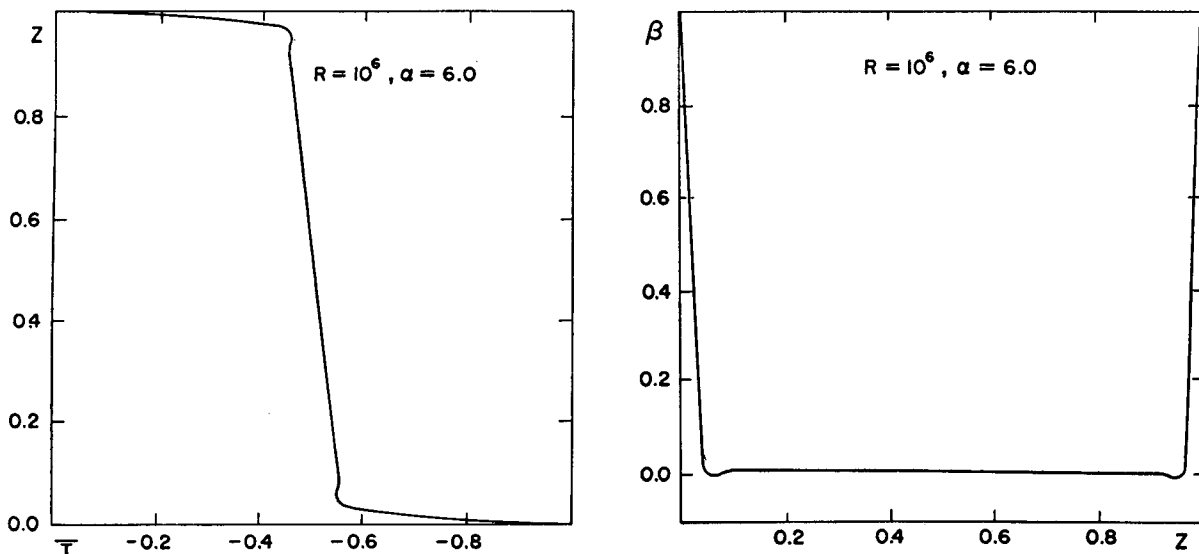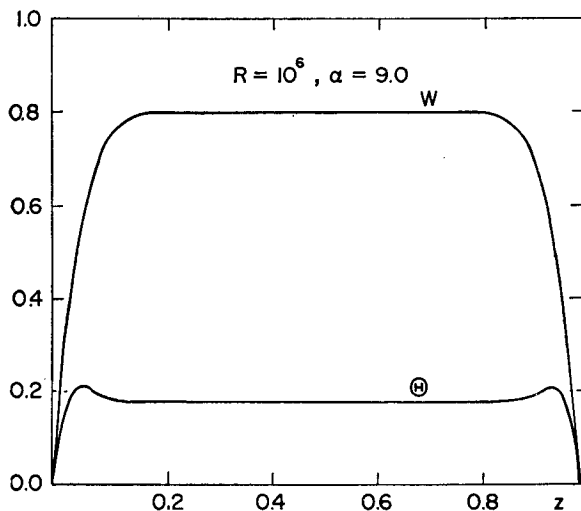$$\times (\bar{\beta}_n - \bar{\beta}_{n+1})^2 + \cdots . \quad (19)$$

This series for R^{-1} converges rather rapidly for all the $\bar{\beta}_n$ which have been computed, and the terms explicitly written in (19) give R to an accuracy of $\lesssim 20$ per cent at $R = 10^6$. We note that for this equation to balance at large R, $\bar{\beta}_1$ must approach 2, and the remaining lower modes must decrease rather slowly as n increases.

Fig. 10. $3.22 \times 10^{-3}w$ and 8.57θ for $R = 10^6$ and $\alpha = 6.0$.

The computed spectra (Fig. 14) are qualitatively quite different from the one derived by Malkus (1954, p. 200). His spectrum is given by

$$\bar{\beta}_n = 2\left(1 - \frac{n}{2n_0 + 1}\right).$$

Here $2n_0 + 1$ is a cut-off in the $\bar{\beta}_n$ spectrum, and it is the total heat flux in our units. Marginal stability is achieved at a much lower Rayleigh number for this spectrum than for the ones computed here.

FIG. 11(a). Mean temperature, $\bar{T}(z)$, for $R = 10^6$ and $\alpha = 6.0$.

FIG. 11(b). Mean gradient, $\beta(z)$, for $R = 10^6$ and $\alpha = 6.0$. $\beta(z)$ is normalized by the total heat transport, $N = 22.3$.

FIG. 12. $1.06 \times 10^{-2} w$ and 12.9θ for $R = 10^6$ and $\alpha = 9.0$.

With regard to the Malkus theory, Figs. 10 and 11 are relevant. For this case ($R = 10^6$, $\alpha = 6.0$) the temperature gradient is everywhere positive except near the boundaries where it approaches zero. The fields in Figs. 10 and 11 therefore fulfill all the requirements of the Malkus theory as formulated by Spiegel (1962). We note for this case that the total heat flux is ~ 22, whereas Malkus obtains a heat transport of ~ 11 for free boundaries. In making this comparison, one should remember that these computations were made for a single horizontal wave number, whereas Malkus presumably allowed for a full spectrum of α's. However, if we interpret the computed heat transport as an upper bound to the heat transport as the Malkus theory prescribes, we con-

clude that for free boundaries the actual upper bound is at least a factor of two larger than that obtained by Malkus.

d) The total heat transport as a function of α and R.
The total heat transport, as a function of R and α is given in Fig. 15. The Rayleigh numbers are indicated in the figure. These curves closely resemble the perturbation calculations at small R, but become increasingly broadened as the Rayleigh number increases. For a given R, the heat transport is entirely conductive ($N = 1$) if α lies outside the bounds prescribed by (18). The value of α which maximizes the heat transport is $1/\sqrt{2}$ at the critical Rayleigh number ($R = 657$), and apparently increases linearly in $R^{\frac{1}{2}}$, at large R. It is well represented at high Rayleigh numbers by the formula:
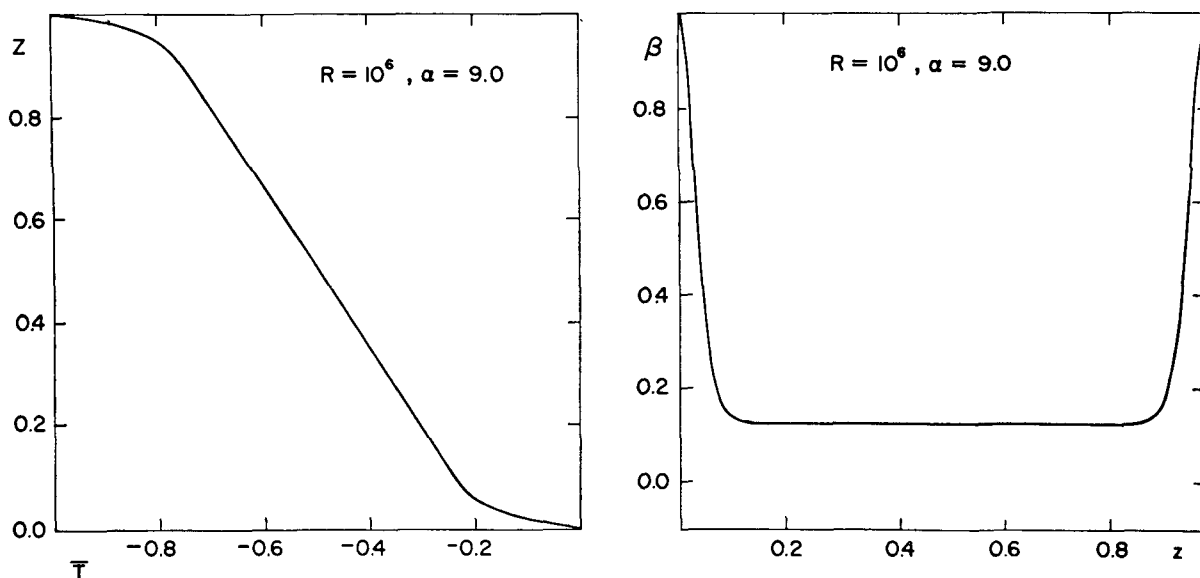
$$\alpha_{max} \simeq 0.7 + 0.01 R^{\frac{1}{2}}. \tag{20}$$

The data on this point is not entirely conclusive because of the large breadth of the curves. It should be pointed out that (20) cannot be a correct asymptotic formula since α_{max} is proportional to $R^{\frac{1}{2}}$ and the value of α beyond which a single α cannot support convection is proportional to $R^{\frac{1}{4}}$ (equation 18).[4] An estimate of the Rayleigh number beyond which (20) is incorrect is not warranted by the accuracy of the curves, but according to (18) and (20), it is $R \gtrsim 10^{18}$.

The maximum heat transport as a function of R is given in Fig. 16. For $R \geq 3000$ the data are accurately represented by the following $R^{\frac{1}{2}}$ law:

$$N \simeq 0.31 R^{\frac{1}{2}}. \tag{21}$$

[4] R. H. Kraichnan has pointed out to the writer that the heat transport, N_{max}, is then asymptotically proportional to $R^{3/10}$.
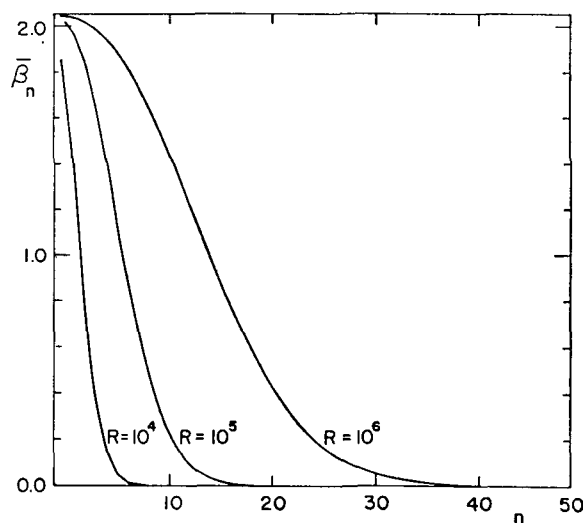
FIG. 13(a). Mean temperature, $\bar{T}(z)$, for $R=10^6$ and $\alpha=9.0$.

FIG. 13(b). Mean gradient, $\beta(z)$, for $R=10^6$ and $\alpha=9.0$. $\beta(z)$ is normalized by the total heat transport, $N=5.40$.

Experimentally, the Nusselt number N is $\sim 0.085R^{\frac{1}{3}}$, for large R, and rigid boundaries (Jakob, 1959). We see no evidence for an intermediate $R^{\frac{1}{4}}$ law, but such a law may only be obtained in the rigid boundary problem. Below $R \sim 10^3$, the data fits smoothly to the perturbation calculation of Malkus and Veronis (1958).

The discrepancy between (21) and the experiment is partly a result of eddy processes which our procedure omits. The use of rigid boundary conditions may improve the agreement, but if (21) is corrected for boundary effects as done by Malkus (1960) by decreasing N by $(657/1107)^{\frac{1}{3}}$, there remains a discrepancy of a factor of 2. If we choose horizontal wave numbers such that the mean gradient is everywhere positive (Figs. 10 and 11) the discrepancy is reduced to 1.8. The latter fields, however, have the unattractive feature of having a large temperature gradient in the central region of the fluid.

5. Linear stability of the fields

The velocity and temperature fields we have so far discussed are stable against the introduction of a disturbance of the *same* horizontal wave number for which the fields were computed. This stability is inherent in the method of integrating the equations. The stability of the steady state amplitudes against disturbances at wave numbers α' other than that α which supports the convection process has not yet been assured in our calculations. The question of stability of the solutions against disturbances of finite amplitudes leads directly back to the multi-α system of equations (13), (14) and (15). We should assume a whole spectrum of α's are initially excited, let them evolve to steady state, and

FIG. 14. Cosine spectrum of the mean temperature gradient for $R=10^4$, 10^5, 10^6 and $\alpha=1.5$.

repeat the calculation for an ensemble of initial conditions. We shall be content here with an investigation of linear stability of the system. This problem has some intrinsic interest, but our main purpose is to lay the framework for an investigation of the multi-α system.

It is convenient to pose the linear stability problem in terms of the Fourier amplitudes [equations (13), (14) and (15)]. We suppose that the system $w_n^{\alpha_1}$, $\theta_n^{\alpha_1}$ and β_n have their steady state values, introduce disturbances δw_n^{α}, $\delta \theta_n^{\alpha}$ and $\delta \beta_n$ and ask whether the latter grow or decay. Since α_1 and α are not coupled, $\delta \beta_n$ must decay initially. The problem then is reduced to determining
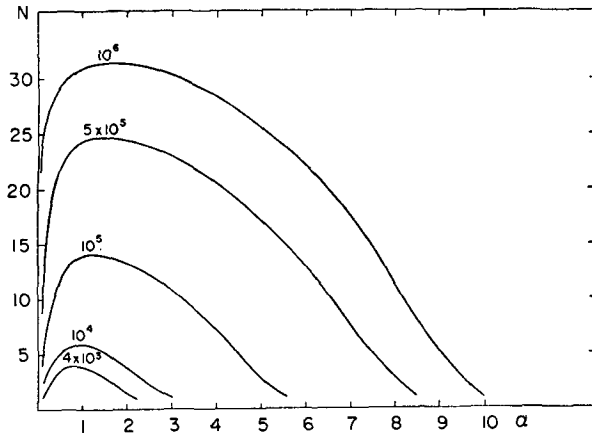
FIG. 15. The total heat transport N as a function of α for
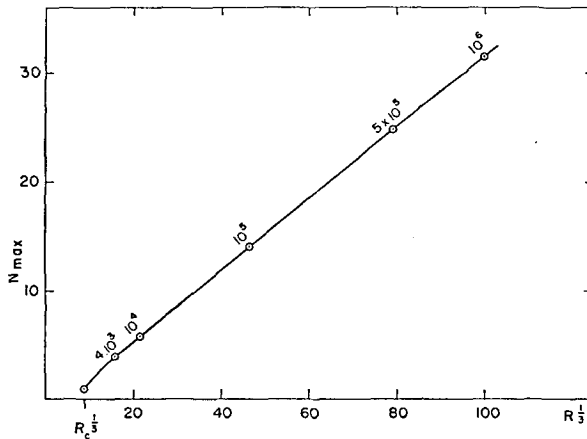$R = 4 \times 10^3$, 10^4, 10^5, 5×10^5 and 10^6.

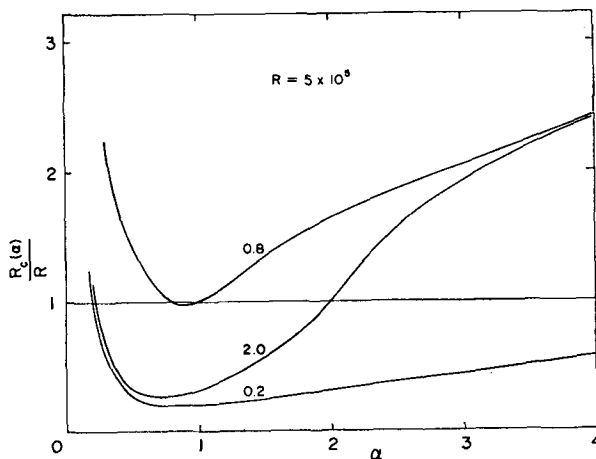FIG. 16. Maximum total heat transport, N_{max} as
a function of $R^{1/3}$.

FIG. 17. Critical Rayleigh number R_c for $R = 5 \times 10^5$ as a function α. The value of α which supports the mean temperature fields labels the various curves.

the growth rates for $\delta w_n{}^\alpha$ and $\delta\theta_n{}^\alpha$ in the presence of the mean gradient β_n. Since exchange of stabilities has been proved for this system (Spiegel, 1962) we know that the system $w_n{}^{\alpha 1}$, $\theta_n{}^{\alpha 1}$, and β_n will be stable if the smallest critical Rayleigh number R_c for the perturbation system, $\delta w_n{}^\alpha$, $\delta\theta_n{}^\alpha$ is larger than the Rayleigh number for which $w^{\alpha 1}$ and $\theta^{\alpha 1}$ were computed.

The marginally stable amplitude $\delta w_n{}^\alpha$, and $\delta\theta_n{}^\alpha$ satisfy (13) and (15) at a Rayleigh number R_c, with the time derivatives put equal to zero. Since the smallest R_c takes an eigen function even about $z = \frac{1}{2}$, we may abbreviate the perturbation system by eliminating the even sine modes from the velocity and temperature fluctuations. Defining

$$\varphi_n = \delta w_{2n-1},$$
$$\varphi_n = \delta w_{2n-1},$$
$$\bar{\beta}_n = \beta_{2n},$$

we may eliminate $\delta\theta_n$ by using the steady state form of (13) and write the marginally stability problem in the following matrix form:

$$A(\bar{\beta})\varphi = \mu\varphi, \qquad (22)$$

where

$$A(\bar{\beta}) = \frac{\alpha^2}{[(2n-1)^2 + \alpha^2]^3}\{\delta_{nm} + \tfrac{1}{2}(\bar{\beta}_{|n-m|} - \bar{\beta}_{n+m-1})\},$$

$$\mu = \frac{\pi^4}{R_c}, \quad \bar{\beta}_0 = 0.$$

In writing the matrix A, we have used the alternative form for the convolution term in (14).

The largest eigen value, μ (smallest R_c), of (22) may be obtained by the matrix iteration technique (Hildebrand, 1952). Since the first sine mode of the velocity will be largest, we may conveniently begin the iteration on a vector containing only this mode. Defining

$$|1\rangle = (1,0,0,\cdots,0,\cdots)$$

we may write

$$\frac{\pi^4}{R_c(\alpha)} = \mu_{max} = \lim_{n\to\infty} \frac{\langle 1|A^n|1\rangle}{\langle 1|A^{n-1}|1\rangle}. \qquad (23)$$

The convergence of the iteration scheme is quite rapid because of the structure of the A matrix. At the highest Rayleigh number considered, $R = 10^6$, the 11th iteration gives R_c to one part in 10^6.

The calculated $R_c(\alpha)$'s are shown in Fig. 17 for $R = 5 \times 10^5$. The particular α which supports the mean field, β, labels the various curves. At low Rayleigh numbers ($R < 5.10^3$) these curves closely resemble those produced by perturbation calculations. Above $R \sim 10^5$

they become increasingly distorted; steady state amplitudes of small horizontal wave numbers are enormously unstable with respect to an introduction of a disturbance at large α.

In Figs. 18 and 19 we give the zones of instability for the computed amplitudes for $R=10^4$ and $R=5\times10^5$. In these graphs, α_1 is the wave number that supports the convective process, and α_2 is the wave number of the perturbation amplitudes. The regions of instability are indicated by the shaded areas, whose outer boundaries are lines of marginal stability. The line $\alpha_1=\alpha_2$ is a trivial case of marginal stability. The value of α at which the two curves cross represents a solution which is infinitesimally stable against all other α's. This value of α begins at $1/\sqrt{2}$ at the critical Rayleigh number and increases slowly with increasing R. The rate of increase is seen to be slower than that α which maximizes the total heat transport. Referring to Fig. 15 we see that the use of the most stable α instead of α_{max} will not appreciably change the total heat transport.

The zones which linear stability theory predicts must have two or more α's supporting convection are indicated by the cross-hatched regions shown in Figs. 18 and 19. These regions are obtained by perturbing the α_1 fields at α_2, assuming that the α_2 field subsequently dominates the convection, and then demanding that the α_2 fields be unstable with respect to a perturbation at α_1. The cross-hatched region is then bounded by the descending marginally stable curve and its reflection about the 45 deg line. At small Rayleigh number, $R<4\times10^3$, this area vanishes but it gradually increases with Rayleigh number.

6. Concluding remarks

The temperature and velocity fields computed here with the fluctuating self-interactions absent show qualitatively a reasonable behavior. The boundary-layering of the temperature field, which is found experimentally, is faithfully reproduced by the system, and the heat transport has the experimentally determined dependence on Rayleigh number. In this respect, our results for the velocity and temperature amplitudes, as well as the stability analysis of the fields, confirm the original ideas of Malkus. However, our result for the heat transport for free boundary conditions does not agree quantitatively with Malkus.

The only disquieting features of the results are the negative temperature gradients which can occur near the boundary for small α, and the rather large amount of heat transported by the system. Aside from eddy processes, there are two other modifications in the system which must be explored before its quantitative accuracy can be properly accessed.

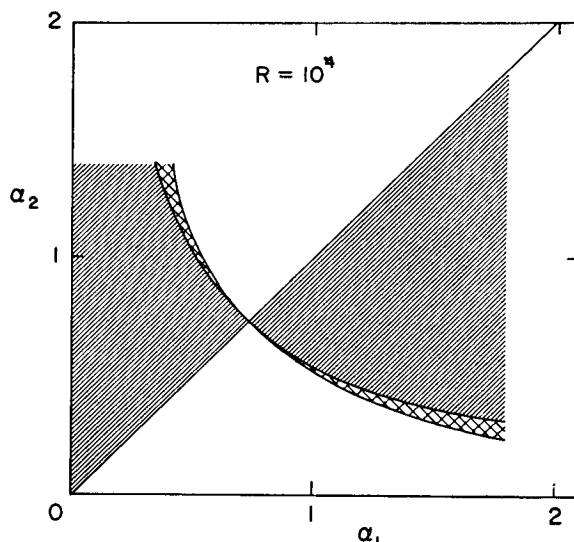First, the use of the more realistic rigid boundary conditions will enable one to examine quantitatively the

FIG. 18. Stability diagram for $R=10^4$. α_1 is the wave number that supports convection, and α_2 is the wave number at which a small perturbation is introduced. The shaded region indicates instability.

FIG. 19. Stability diagram for $R=5\times10^5$. α_1 is the wave number that supports convection, and α_2 is the wave number at which a small perturbation is introduced. The shaded regions indicate instability.
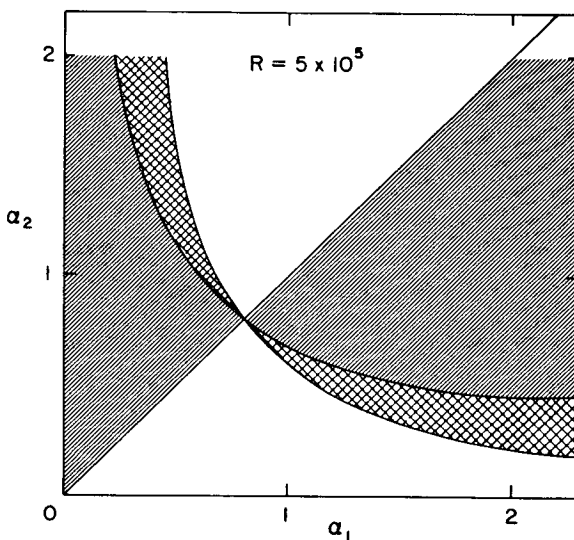
role of the eddy processes in producing the experimental temperature profile and the total heat flux. The presence of shear forces at the boundary will decrease the computed heat flux, and in checking the development of large scale horizontal motions there, it will reduce the negative temperature gradient. Preliminary indications are that the use of rigid-boundary conditions decrease the total heat transport by a factor of 2.3. Secondly, the introduction of several horizontal wave numbers will

make the system more realistic, particularly at large Rayleigh numbers. It will also permit a study of finite amplitude stability of the system. The above modifications are currently under investigation and will be reported on in the near future.

Acknowledgments. The author is very grateful to Dr. R. H. Kraichnan for suggesting this investigation, for many illuminating discussions through the completion of the work, and for making helpful suggestions regarding the presentation of material. He is also grateful to Dr. E. A. Spiegel for many valuable discussions, and for critically reading a final version of the manuscript.

It is a pleasure to acknowledge the able assistance of Mr. R. Rustin, who programmed and carried out the numerical computations on the IBM 7090 computer.

REFERENCES

Chandrasekhar, S., 1961: *Hydrodynamic and hydromagnetic stability.* Oxford, Clarendon Press, p. 16.

Deissler, R. G., 1962: Turbulence in the presence of a vertical body force and temperature gradient. *J. geophys. Res.,* **67**, 3049–3062.

Hildebrand, F. B., 1952: *Methods in applied mathematics.* Englewood Cliffs, N. J., Prentice-Hall, Inc., p. 66 *et. seq.*

Jakob, M., 1959: *Heat transfer.* Vol. 1, New York, John Wiley and Sons, Inc., p. 535.

Kraichnan, R. H., 1962a: Turbulent thermal convection at arbitrary Prandtl Number. *Phys. Fluids,* **5**, 1374–1389.

——, 1962b: The closure problem of turbulence theory. *Proceedings of symposia in applied mathematics: Vol. 13, Hydrodynamic instability,* Providence, R. I., Amer. Math. Soc., 199–225.

Kuo, H. L., 1961: Solution of the nonlinear equations of cellular convection and heat transport. *J. fluid Mech.,* **10**, 611–634.

Malkus, W. V. R., 1954: The heat transport and spectrum of thermal turbulence. *Proc. Roy. Soc. London,* A, **225**, 196–212.

——, 1960: Turbulence, notes of summer study program in geophysical fluid dynamics at the Woods Hole Oceanographic Institution. Unpublished, p. 38 *et seq.*

——, and G. Veronis, 1958: Finite amplitude cellular convection. *J. fluid Mech.,* **4**, 225–260.

Ogura, Y., 1962: Energy transfer in an isotropic turbulent flow. *J. geophys. Res.,* **67**, 3143–3150.

Saltzman, B., 1961: Finite amplitude free convection as an initial value problem. *J. atmos. Sci.,* **19**, 329–341.

Spiegel, E. A., 1962: On the Malkus theory of turbulence. *Mechanique de la Turbulence,* Paris, C. N. R. S., 181–201.